J|A|C|S
ARTICLES
Published on Web 03/14/2003

# Conformation and Luminescence of Isolated Molecular Semiconductor Molecules

Melissa A. Summers, Paul R. Kemper, John E. Bushnell, Matthew R. Robinson, Guillermo C. Bazan, Michael T. Bowers, and Steven K. Buratto*

*Contribution from the Department of Chemistry and Biochemistry, University of California, Santa Barbara, Santa Barbara, California 93106-9510*

Received August 21, 2002; E-mail: buratto@chem.ucsb.edu

***Abstract:*** In this article, we describe, for the first time, direct comparisons of the detailed structures of two small molecule organic semiconductors, oligo(phenylenvinylene) (OPV) molecules with chains of five and six phenyl rings (5R-$OC_8H_{17}$ and 6R-$OC_8H_{17}$), respectively, and their luminescence properties on a single molecule level. Our data originate from a combination of two powerful diagnostic tools in physical chemistry: ion mobility and single molecule fluorescence spectroscopy. These techniques enable us to precisely determine the shapes of isolated molecules in the gas phase and to correlate these structures to the emission from single molecules supported on bare glass substrates. The principal structural uncertainty in OPVs is the (possible) presence and location of cis-vinylene linkages (cis-defects) in the oligomer. The results show that the structures observed in the gas phase are strongly correlated to the categories of molecules observed in the single molecule polarization anisotropy measurements with nearly identical distributions for the two OPV molecules studied. Each category is also characterized by the luminescence efficiency of the molecules in each class, providing a direct correlation between the luminescence efficiency and the shape of the molecule. This combination of techniques provides a level of information far beyond that obtained via any other analytical technique.

The promise of versatile, low-cost optoelectronics from organic molecules has spurred widespread interest in the synthesis of new molecular semiconductors. A trend that has recently emerged in this field is the so-called "oligomer approach"[1−3] in which low and intermediate molecular weight organic molecules with high luminescence quantum yields are synthesized to serve as the active layer in optoelectronic devices such as organic light-emitting diodes (OLEDs) and lasers. Unlike many conjugated polymers used in optoelectronic devices, these molecules are high in purity and well-defined. They can be tailor-made with functional groups to render them soluble for ease of processing and with novel geometries that allow control over film morphology.[3] Furthermore, oligomers have been synthesized to serve as model compounds for polymers, in part because their structure and intermolecular interactions can be controlled more precisely, eliminating the uncertainty inherent in polymers (Scheme 1).[4−7]

***Scheme 1.*** All Trans Structures of 5R-$OC_8H_{17}$ and 6R-$OC_8H_{17}$

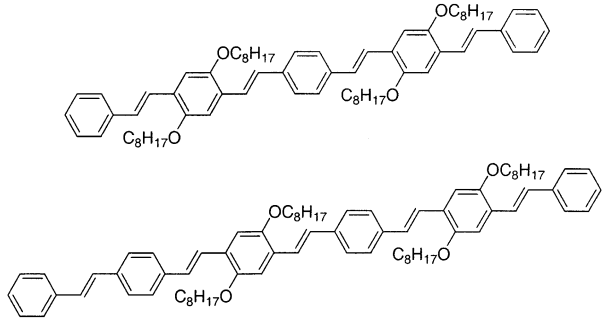


While this approach to new materials has shown promise, typical applications of these molecules in device components involve amorphous thin films in which the molecular subunits experience a range of environments and have poorly defined morphological irregularities.[8] Furthermore, because intermolecular energy migration is facile in the bulk, the optical properties under study may be dominated by only a small fraction of the sample.[9] Thus, the structural (conformational) purity of these molecules is of paramount importance, but determining this property is difficult, and it is not known in general. Although nuclear magnetic resonance (NMR) can reveal the presence and amount of cis-defects, NMR cannot yield information about where the defects occur or how they affect the shape of the oligomer.[16] By probing the optical properties

(1) Robinson, M. R.; Wang, S.; Bazan, G. C.; Cao, Y. *Adv. Mater.* **2000**, *12*, 1701.
(2) Oldham, W. J., Jr.; Lachicotte, R. J.; Bazan, G. C. *J. Am. Chem. Soc.* **1998**, *120*, 2987.
(3) Robinson, M. R.; Wang, S.; Heeger, A. J.; Bazan, G. C. *Adv. Funct. Mater.* **2001**, *11*, 413.
(4) Cornil, J.; dos Santos, D. A.; Crispin, X.; Silbey, R.; Bredas, J. L. *J. Am. Chem. Soc.* **1998**, *120*, 1289.
(5) Gebhardt, V.; Bacher, A.; Thelakkat, M.; Stalmach, U.; Meier, H.; Schmidt, H.-W.; Haarer, D. *Adv. Mater.* **1999**, *11*, 119.
(6) Oelkrug, D.; Tompert, A.; Gierschner, J.; Egelhaaf, H.-J.; Hanack, M.; Hohlock, M.; Steinhuber, E. *J. Phys. Chem. B* **1998**, *102*, 1902.
(7) Peeters, E.; Ramos, A. M.; Meskers, S. C. J.; Janssen, R. A. J. *J. Chem. Phys.* **2000**, *112*, 9445.
(8) Renak, M.; Bartholomew, G. P.; Wang, S.; Ricatto, P. J.; Lachicotte, R. J.; Bazan, G. C. *J. Am. Chem. Soc.* **1998**, *121*, 7787.
(9) Guillet, J. *Polymer Photophysics and Photochemistry*; Cambridge University Press: Cambridge, U.K., 1985.

of isolated single oligomers, however, it is possible to establish structure−property relationship trends and use these findings to understand the properties of more complex materials, such as polymers, dendrimers, and other related macromolecules. Revealing the relationship between the shapes of these oligomers and their optical properties is the first step in understanding how to control the optical properties of thin organic films.

Insight into the dependence of molecular shape on the luminescence properties of individual molecules can be obtained from single molecule fluorescence measurements. Over the past five years, there have been several reports of single molecule fluorescence studies of molecular semiconductors including conjugated polymers, dendrimers, and other small luminescent organic molecules.[10−15] While these initial studies have yielded important new fundamental insights into the luminescence properties, there have been no *direct* comparisons between the luminescence and the detailed structure of the molecule. The principal reason for this is that the single molecule fluorescence data alone are not sufficient to determine the structure of the molecule and a complementary technique is required.

Over the past seven years, ultrasensitive optical detection techniques have made possible spectroscopy of single molecules at room temperatures and have allowed the observation of phenomena otherwise obscured in ensemble measurements such as discrete fluctuations in intensity, spectral wandering, and fluctuations in the dipole orientation.[17,18] In the experiments described here, we probe the luminescence of single oligomers as a function of the exciting light polarization.

Single molecule fluorescence anisotropy measurements suggest that the OPV molecules fall into discrete categories, depending on the conformation adopted by the individual molecule. The polarization anisotropy of the molecules in each category can then be compared to the detailed structures provided by the gas-phase ion mobility measurements. The results show that the structures observed in the gas phase are strongly correlated to the categories of molecules observed in the single molecule fluorescence measurements with nearly identical distributions for the two OPV molecules studied. In addition, each category is characterized by the emission intensity of the molecules in each class, providing a correlation between the luminescence efficiency and the shape of the molecule. Finally, we show that the number and location of cis-defects strongly correlate with the shape of the molecule. We see no evidence of tetrahedral (i.e., $sp^3$ carbon atom) defects in either of our molecules by mass spectrometry, as has been previously suggested as a bending defect in the polymer MEH-PPV.[10]

Figure 1 shows an image of single 6R-$OC_8H_{17}$ molecules dispersed on a glass coverslip acquired using our home-built laser scanning confocal microscope. Samples are prepared by spin-casting (30 $\mu$L aliquot) from ∼0.1 nM oligomer solution in toluene to ensure an average spacing between molecules of at least 1 $\mu$m. A fluorescence image is acquired by rastering the sample using a four quadrant piezo tube driven by commercial scanning electronics.[19,20] All experiments are performed in a pure $N_2$ atmosphere, and care is taken to remove oxygen from the sample chamber.[21] Our apparatus allows us to position the excitation spot over a selected molecule and acquire the total fluorescence as a function of time and polarization anisotropy simultaneously as shown in Figure 2. An electrooptic modulator (EOM) in combination with a quarter-wave plate allows us to rotate the linear polarization of the excitation laser through 180° at a fixed frequency. A molecule with a net absorption dipole (or anisotropic polarizability tensor) will

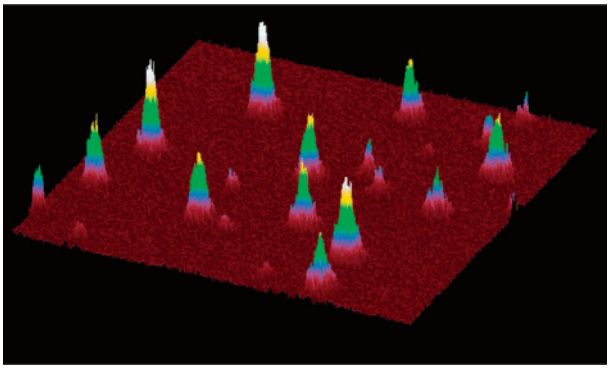

***Figure 1.*** Side view of a 9 $\mu$m$^2$ laser scanning confocal microscopy image, showing the intensity and position of single 6R-$OC_8H_{17}$ molecules dispersed on a bare glass surface. The maximum (white) intensity corresponds to ∼10 kcps.

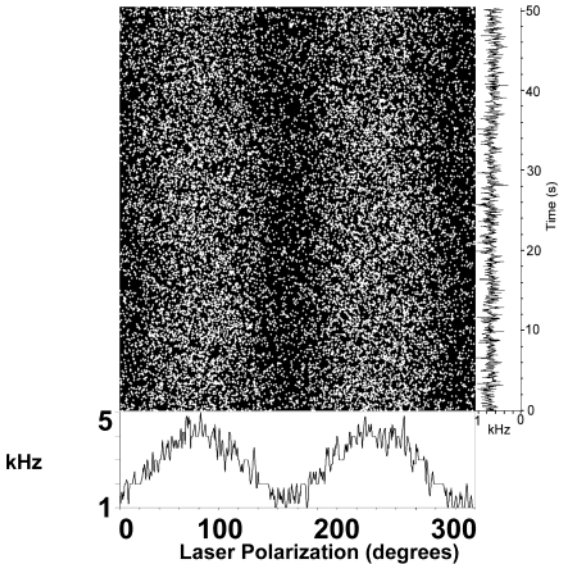


***Figure 2.*** Polarization modulation data, in image format, of a 5R-$OC_8H_{17}$ single molecule. The *x*-axis of the image corresponds to the (arbitrary) orientation of the linear laser polarization. The laser polarization is modulated at a frequency of ∼20 rotations ($s^{-1}$); therefore, the *x*-axis corresponds to $\sim 1/20$ s. The trace shown below the image is the average intensity along the *y*-axis, showing a pronounced sinusoid characteristic of a molecule with a well-defined polarizability axis. Averaging along the *x*-axis yields a 50-s intensity trajectory, seen to the right of the image.

(10) Hu, D. H.; Yu, J.; Wong, K.; Bagchi, B.; Rossky, P. J.; Barbara, P. F. *Nature* **2000**, *405*, 1030.
(11) White, J. D.; Hsu, J. H.; Fann, W. S.; Yang, S.-C.; Pern, G. Y.; Chen, S. A. *Chem. Phys. Lett.* **2001**, *338*, 263.
(12) Lu, H. P.; Iakoucheva, J. M.; Ackerman, E. J. *J. Am. Chem. Soc.* **2001**, *123*, 9184.
(13) Weston, K. D.; Goldner, L. S. *J. Phys. Chem. B* **2001**, *105*, 3453.
(14) Hofkens, J.; Vosch, T.; Maus, M.; Kohn, F.; Cotlet, M.; Weil, T.; Herrmann, A.; Mullen, K.; De Schryver, F. C. *Chem. Phys. Lett.* **2001**, *333*, 255.
(15) Deschenes, L. A.; Vanden Bout, D. A. *Science* **2001**, *292*, 255.
(16) Wind, M.; Weisler, U.-M.; Saalwachter, K.; Mullen, K.; Spiess, H. W. *Adv. Mater.* **2001**, *13*, 752.
(17) Xie, X. S.; Trautman, J. K. *Annu. Rev. Phys. Chem.* **1998**, *49*, 441.
(18) Moerner, W. E.; Orrit, M. *Science* **1999**, *283*, 1670.
(19) Weston, K. D.; Carson, P. J.; Metiu, H.; Buratto, S. K. *J. Chem. Phys.* **1998**, *109*, 7474.
(20) Weston, K. D.; Carson, P. J.; DeAro, J. A.; Buratto, S. K. *Chem. Phys. Lett.* **1999**, *58*, 308.
(21) Sirbuly, D. J.; Mason, M. D.; Schmidt, J. P.; Summers, M. A.; Buratto, S. K. *Rev. Sci. Instrum.*, submitted.

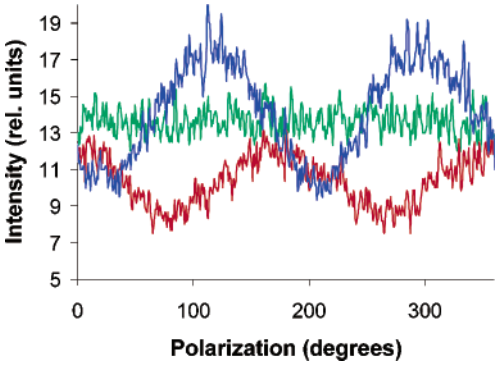


***Figure 3.*** Polarization modulation traces for three molecules corresponding to the three categories of 5R-$OC_8H_{17}$ molecules observed: elongated, bent, and kinked. The three molecules were excited with nearly the same laser intensity.

exhibit a sinusoidal intensity trajectory as seen on the horizontal axis in Figure 2.[22] The time course (the vertical axis in Figure 2) shows a single intensity level that indicates the molecule is emitting with no interruptions in a single "on" level. In the absence of air, we have observed continuous emission for several minutes from these molecules. The anisotropy in the polarizability is inferred from the depth-of-modulation of the sinusoid in Figure 2. For this particular molecule, the depth-of-modulation is 0.9, indicating a large anisotropy consistent with an elongated OPV, which is expected for a molecule with all trans-vinylene linkages. We note that it is possible to obtain the orientation of the molecule by comparing the phase of the sinusoid to the phase of the modulation of the exciting light by the EOM. For our samples which are prepared by spin-casting, the molecules are *all* randomly oriented in the plane of the surface. We observe no molecules with the polarization component along the surface normal as observed using methods described elsewhere.[23,24] The distribution of polarization anisotropy and the distribution of fluorescence intensity are obtained from the single molecule statistics (roughly 100 single molecules were sampled for both 5R-$OC_8H_{17}$ and 6R-$OC_8H_{17}$).

Figure 3 shows the polarization anisotropy for three 5R-$OC_8H_{17}$ molecules. These three molecules represent the three classes of behavior observed for this compound. A large polarization anisotropy is represented by the blue trace which has a depth-of-modulation = 1.0, a small polarization anisotropy is represented by the red trace (DOM = 0.4), and an isotropic polarization is represented by the green trace (DOM = 0.0). We attribute these signals to classes of molecules that are completely elongated (green), bent (red), or strongly kinked (green). These three

***Table 1.*** Comparison of Ion Mobility and Single Molecule Spectroscopy Populations for 5R-$OC_8H_{17}$

| 5R-$OC_8H_{17}$ | | |
|---|---|---|
| conformation | ion mobility percentage | SMS percentage |
| all trans | 59.0 | 71 |
| cis (1) [or cis (4)] | 17.8 | |
| cis (2) [or cis (3)] | 9.5 | 19 |
| cis (1, 2) [or cis (3, 4)] | 3.0 | |
| cis (1, 4) | 5.3 | |
| cis (1, 3) [or cis (2, 4)] | 3.0 | 10 |
| cis (2, 3) | 2.4 | |

classes of molecules can also be characterized by the peak luminescence intensity that is highest for the elongated molecules and lowest for the kinked molecules, more than a 75% difference in intensity on average with a standard deviation of 10%.

Histograms of the fractional polarization anisotropy for 104 5R-$OC_8H_{17}$ and 93 6R-$OC_8H_{17}$ single molecules are presented in Figure 4. The DOM histogram for the 5R-$OC_8H_{17}$ molecules shows three distinct categories of DOM, DOM < 0.3, 0.3 < DOM < 0.7, and 0.7 < DOM, which correspond to the green, red, and blue traces of Figure 3, respectively. The DOM histogram of the 6R-$OC_8H_{17}$ molecules is clearly different than that of the 5R-$OC_8H_{17}$ molecules. For this system, the population of the molecules with DOM < 0.45 is larger than that of molecules with 0.45 < DOM < 0.7.

This histogram can be separated into three or four DOM categories. We choose four categories, DOM < 0.25, 0.25 < DOM < 0.5, 0.5 < DOM < 0.75, and DOM > 0.75, to be consistent with the structures observed in the gas-phase experiments described below. The percentages of each DOM category are listed in Tables 1 and 2 under the SMS heading for the 5R-$OC_8H_{17}$ and 6R-$OC_8H_{17}$ molecules, respectively. We are then able to compare these assignments of classes of molecules with the detailed structures obtained in the gas-phase experiments described below.

To determine the distribution of structural isomers in a given synthetic batch, ion mobility based ion chromatography experiments are performed.[25−27] In these experiments, a sample is dissolved in a solvent, and a thin layer is deposited on a cylindrical surface. The OPVs are desorbed and photoionized by a 10 ns laser pulse from a nitrogen laser operating at 337 nm. The pulse of ions is mass selected and injected at low energy into a cylindrical cell filled with several Torr of He gas. The ions drift through the cell under the influence of a weak electric

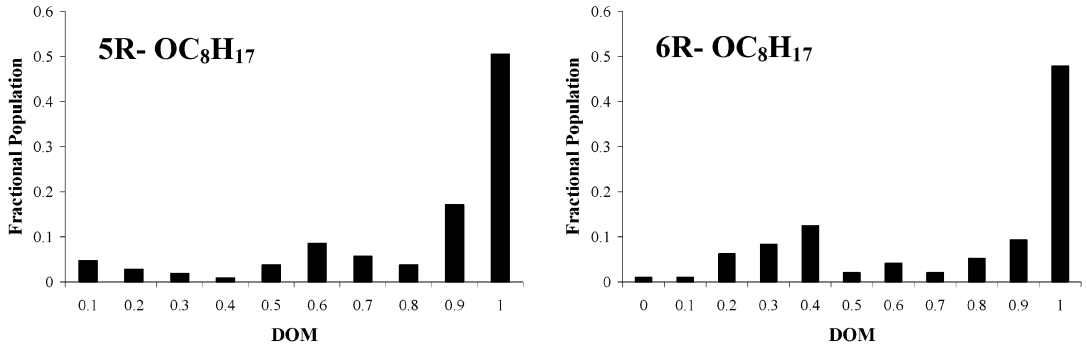


***Figure 4.*** Depth of modulation (DOM) histograms for the 5R-$OC_8H_{17}$ and 6R-$OC_8H_{17}$ molecules. Three distinct peaks are observed in the case of the 5R-$OC_8H_{17}$ molecules which correlate to the DOMs shown in Figure 3. The histogram for the 6R-$OC_8H_{17}$ molecules is skewed to the lower DOM values. Statistics derived from these histograms are reported in Tables 1 and 2, respectively.

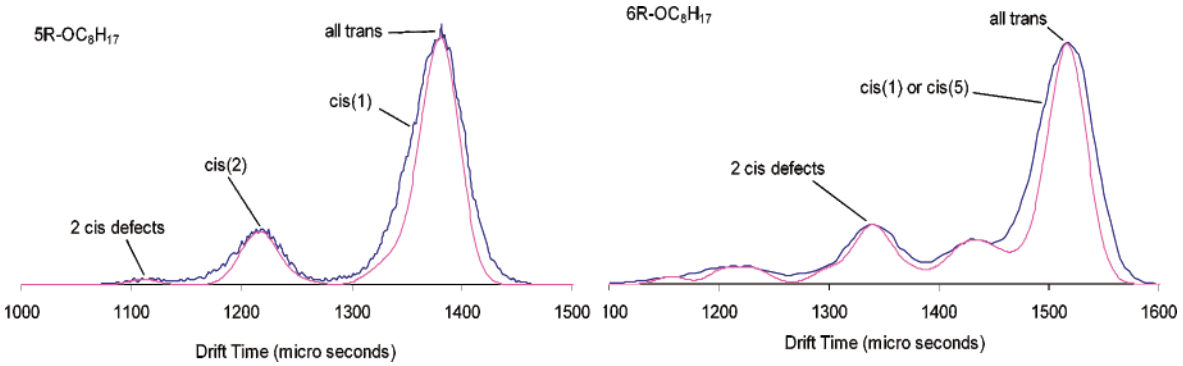


***Figure 5.*** Experimental arrival time distributions (blue traces) for the parent cations of 5R-$OC_8H_{17}$ and 6R-$OC_8H_{17}$. The pink traces are a fit to the data using theoretical cross sections of various isomers of the two systems. The resulting isomer percentages of 5R-$OC_8H_{17}$ and 6R-$OC_8H_{17}$ are reported in Tables 1 and 2, respectively.

***Table 2.*** Comparison of Ion Mobility and Single Molecule Spectroscopy Populations for 6R-$OC_8H_{17}$

| 6R-$OC_8H_{17}$ | | |
|---|---|---|
| conformation | ion mobility percentage | SMS percentage |
| all trans | 53.2 | 65 |
| cis (1) + cis (5) | 11.2 | |
| cis (2) + cis (4) | 10.0 | 6 |
| cis (3) | 4.4 | |
| cis (1, 2) + cis (4, 5) | 4.0 | 21 |
| cis (1, 5) | 2.7 | |
| cis (2, 3) + cis (3, 4) | 4.0 | |
| cis (1, 3) + cis (3, 5) | 4.0 | |
| cis (2, 4) | 2.7 | 8 |
| cis (1, 4) + cis (2, 5) | 4.0 | |

field, pass through a quadrapole mass filter, and are detected. Because this is a pulsed experiment, arrival time distributions (ATDs) are obtained, which yield mobilities, which in turn yield collision cross sections.[28] If several structural isomers exist in the mass selected beam, then the more compact isomer reaches the detector first (highest mobility, lowest cross section), and the less compact ions arrive at longer times proportional to their cross sections. In the case of the OPV molecules, we feel the ionic gas-phase structural distributions should accurately map the condensed phase distribution for the following reasons. The ions are formed by photoionization during the laser pulse, and because two photon ionization is near resonant,[29] cold molecular ions are formed. The barrier to cis/trans isomerization is of the order of 50 kcal/mol in stilbene[30] (two phenyls connected by a vinyl group) and should not occur in these cold ions. When pure cis- or trans-stilbene is used in the experiment, the corresponding ATDs contain only pure cis- or trans-stilbene indicating ionization, and subsequent travel through the instrument does not induce isomerization. As the chain length increases, the cis/trans isomerization barrier increases as well, further reducing the likelihood of isomerization. Comparison of the ion mobility results with the single molecule photophysics experiments is in accord with our expectations (see Tables 1 and 2).

The experimental ATDs for 5R-$OC_8H_{17}$ and 6R-$OC_8H_{17}$ are given in Figure 5 as the blue lines. In the 5R-$OC_8H_{17}$ ATD, at least three resolved features are observed, and in the 6R−$OC_8H_{17}$ ATD, at least four resolved features are observed. These data on their own indicate that multiple structural isomers exist in both instances. If the all trans isomer is present, it must occur as (part of) the peak at the longest times because it has the largest rotationally averaged cross section. The peaks at shorter times must then have one or more cis-defects leading to folding of the OPV and more compact structures.

While this qualitative information is useful, much more detailed structural information can be obtained from computer modeling. For the molecules discussed here, we used the AMBER force field[31] for MM/MD calculations and a previously developed annealing protocol[32] to generate approximately 100 low energy structures for all possible cis/trans isomers of both 5R-$OC_8H_{17}$ and 6R-$OC_8H_{17}$. Several low energy structures of each isomer were then subjected to 1 ns dynamics at 300 K with cross sections obtained at 1 ps intervals (1000 in all). These were then averaged to get a cross section for that isomer. An arrival time was then determined for each isomer, and the experimental ATDs in Figure 5 for 5R-$OC_8H_{17}$ and 6R-$OC_8H_{17}$ were fit to obtain isomer distributions.

These fits are plotted as the pink curves in Figure 5. Clearly, both fits are excellent. The percentages of each isomer for both OPVs are given in Tables 1 and 2. In Figure 5 and Tables 1 and 2, cis(1) corresponds to a cis-defect in the first vinyl group, cis(2) corresponds to a cis-defect in the second vinyl group, cis(1,2) corresponds to cis-defects in both the first and the second vinyl groups, etc. The horizontal lines in Tables 1 and 2 that stretch into the SMS percentage column represent the group of structures that combine to form the peaks observed in the ATDs. For example, the peaks for the all trans and for the cis(1) [or cis (4)] structures are not resolved and are summed to yield the large peak in the 5R-$OC_8H_{17}$ ATD.

(22) Ha, T.; Enderle, T.; Chemla, D. S.; Selvin, P. R.; Weiss, S. *Phys. Rev. Lett.* **1996**, *66*, 3979.
(23) Fourkas, J. T. *Opt. Lett.* **2001**, *26*, 211.
(24) Bartko, A. P.; Dickson, R. M. *J. Phys. Chem. B* **1999**, *103*, 3053.
(25) von Helden, G.; Hsu, M.-T.; Kemper, P. R.; Bowers, M. T. *J. Chem. Phys.* **1991**, *95*, 3835.
(26) Bowers, M. T.; Kemper, P. R.; von Helden, G.; van Koppen, P. A. M. *Science* **1993**, *260*, 1446.
(27) Bowers, M. T. *Acc. Chem. Res.* **1994**, *27*, 234.
(28) McDaniel, E. W.; Mason, E. A. *The Mobility and Diffusion of Ions in Gases*; Wiley: New York, 1973.
(29) Pedley, J. B.; Rylance, J. *Sussex-NP.L Computer Analyzed Thermochemical Data: Organic and Organometallic Compounds*; University of Sussex, U.K., 1977.
(30) Soltiel, J.; Garapathy, S.; Werking, C. *J. Phys. Chem.* **1987**, *91*, 2755.
(31) Case, D. A.; Pearlman, D. A.; Caldwell, J. W.; Cheatham, T. E., III; Ross, W. S.; Simmerling, C. L.; Darden, T. A.; Merz, K. M.; Stanton, R. V.; Cheng, A. L.; Vincent, J. J.; Crowley, M.; Tsui, V.; Radmer, R. J.; Duan, Y.; Piteva, J.; Massova, I.; Seibel, G. L.; Singh, U. C.; Weiner, P.; Kollman, P. A. AMBER 6.0, University of California at San Francisco, 1999.
(32) Wyttenbach, T.; von Helden, G.; Batka, J. J., Jr.; Carlat, D.; Bowers, M. T. *J. Am. Soc. Mass Spectrom.* **1997**, *8*, 275.

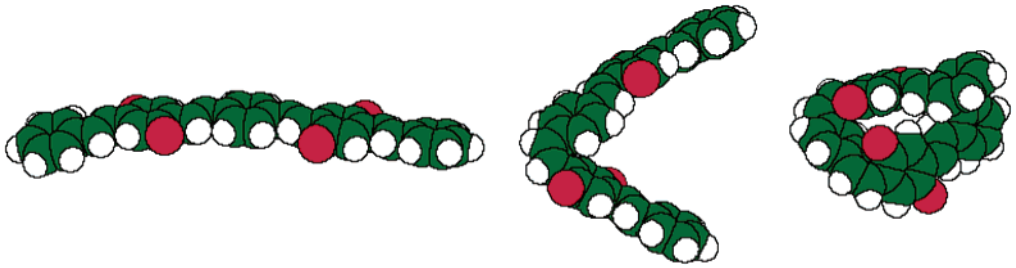

***Figure 6.*** Conformations of the all trans, cis(2), and cis(2,3) isomers of 5R-$OC_8H_{17}$. The $C_8H_{17}$ side chains have been removed for clarity. The green spheres are C atoms, the red spheres are O atoms, and the small white spheres are H atoms.

Several things are apparent from the ion mobility results in the tables. First, the all trans species comprises only 59% of the 5R-$OC_8H_{17}$ isomers and 53% of the 6R-$OC_8H_{17}$ isomers. These two samples were synthesized to maximize the formation of the all trans isomer and subjected to postsynthesis UV radiation to promote isomerization to the all trans isomer. Clearly, forming an isomerically pure all trans sample will take further work. Second, as the oligomer gets larger, more cis-defects occur, especially multiple cis-defects. The dramatic effect of cis-defects on conformation is shown in Figure 6, where the structures of the all trans, cis(2), and cis(2,3) isomers of 5R-$OC_8H_{17}$ are shown. The reason for the large variation in polarization anisotropy observed between isolated single molecules (Figure 3) is now apparent.

Finally, the agreement between the ion mobility and SMS results is remarkable and *implies* that the isolated molecules spin cast on a glass cover slip and interrogated by single molecule fluorescence methods have the same cis/trans isomer distribution as those laser desorbed, ionized, and interrogated by ion mobility methods in the gas phase. This is an extremely important result because it allows quick and definitive isomer distributions to be determined using mass spectrometry/ion mobility methods for synthetic protocols from only trace amounts of materials (nanomoles). These measurements will provide instant feedback to the synthetic group so protocols can be maximized for a desired result. The much more difficult and time-consuming photophysics measurements will only need to be done on promising candidates.

In summary, we present here the results of the synergistic interaction of three different but complementary scientific efforts: synthesis (Bazan group), structure (Bowers group), and photophysical characterization (Buratto group). Together these efforts provide a very realistic strategy for developing photoluminescent materials that should be excellent candidates for organic optoelectronic devices, a process we are actively pursuing.

**Acknowledgment.** We gratefully acknowledge the support of the Air Force Office of Scientific Research under grant F49620-98-1-0048 (to M.T.B.) and the David and Lucille Packard Foundation for a Packard Fellowship (to S.K.B.).

JA028241P